

Anisotropic properties of the excitation spectrum of Sr_2RuO_4 crystals ($T_c=1.4$ K) in the normal state investigated by Raman scattering

Shigenobu Sakita and Shigeki Nimori*

Venture Business Laboratory, Hiroshima University, Kagamiyama 2-313, Higashi-Hiroshima 739-8527, Japan

Zhiqiang Q. Mao and Yoshiteru Maeno

*Department of Physics, Kyoto University, Kyoto 606-8502, Japan**and Core Research for Evolutional Science and Technology, Japan Science and Technology Corporation (CREST-JST), Saitama 332-0012, Japan*

Norio Ogita and Masayuki Udagawa

Faculty of Integrated Arts and Sciences, Hiroshima University, Kagamiyama 1-7-1, Higashi-Hiroshima 739-8521, Japan

(Received 24 July 2000; revised manuscript received 11 October 2000; published 15 March 2001)

We have systematically investigated the totally symmetric Raman-scattering spectra of Sr_2RuO_4 crystals in the temperature region between room temperature and 6 K. The electron-phonon interaction for the apical oxygen vibration has been experimentally investigated by a line-shape analysis based on the Fano interference model. It has been found that the electron-phonon interaction strongly depends on not only the polarization geometry but also the phonon-propagating direction. The phonon, which travels along the RuO_2 plane in the (a,a) geometry, shows the strongest electron-phonon interaction. The intensity of the broad background due to the magnetic excitation has been suppressed in the energy region less than 300 cm^{-1} at low temperature. Furthermore, the anisotropic formation of the spin gap has been also observed in excitation spectra with the propagation vector parallel to the RuO_2 plane below 60 cm^{-1} at 7 K. These anisotropic properties have been obtained for a crystal with a high superconductivity transition temperature of 1.4 K. The sample quality is very important, since such an anisotropic property has not been observed in the Raman spectra for samples with $T_c=0.97$ K. The observed magnetic excitation suggests that the magnetic correlation is also important in understanding the mechanism of superconductivity of Sr_2RuO_4 .

DOI: 10.1103/PhysRevB.63.134520

PACS number(s): 74.25.Kc, 63.20.Kr

I. INTRODUCTION

Sr_2RuO_4 is the first noncopper superconductor with a layered perovskite structure similar to high- T_c cuprates.¹ After the proposal of the spin-triplet pairing by Rice and Sigrist,² the recent extensive experiments of NMR,³ μSR ,⁴ tunneling,⁵ specific heat,⁶ and ac susceptibility⁷ have supported that Cooper-pair symmetry is p wave. Sr_2RuO_4 has the same K_2NiF_4 -type structure as $\text{La}_{2-x}\text{Sr}_x\text{CuO}_4$, which is known as a d -wave superconductor.

For the Raman scattering of Sr_2RuO_4 , we mention a few reports. Udagawa *et al.* reported that there is no anomalous properties for the phonon spectra and the ionic interaction along the c axis is stronger than that of $\text{La}_{2-x}\text{Sr}_x\text{CuO}_4$.⁸ Yamanaka *et al.* estimated the scattering rate of the charge carrier from the structureless continuum spectrum extending to 4000 cm^{-1} .⁹ However, these results were obtained with crystals of relatively low temperature of superconductivity $T_c=0.97$ K. With careful treatment during crystal growth, T_c has been increased up to 1.5 K, which is believed to be close to the intrinsic T_c of Sr_2RuO_4 . Such dramatic change in the sample quality gives us the possibility of obtaining information in Raman scattering. In fact, we have found¹⁰ that the line shape of the apical oxygen vibration in high-quality samples is highly anisotropic and the asymmetric line shape is well explained by the interference model formulated

by Fano.^{11,12} Recently, for $\text{La}_{2-x}\text{Sr}_x\text{CuO}_4$, we have observed similar electron-phonon interaction in the wide carrier-concentration region and have found that the electron-phonon interaction for the apical oxygen vibration at $\sim 440\text{ cm}^{-1}$ correlates with T_c .¹³

Optical reflectivity has been measured by Katsufuji *et al.*¹⁴ From the broad response due to carriers, they have found that the ratio of the in-plane to out-of-plane low-energy spectral weight is about 10^2 and the conduction carriers become coherent along the c axis with decreasing temperature. However, no phonon anomaly was reported in their paper.

The phonon anomaly observed by neutron scattering has been reported by Braden *et al.*¹⁵ Sr_2RuO_4 has a structural instability due to the RuO_6 octahedron rotation about the c axis, as evidenced from the sharp energy drop of phonon dispersion near the zone boundary. However, the structural phase transition due to this instability has not been observed, since its energy does not vanish in the temperature region between room temperature and 12 K.

In this paper, we have studied the polarization and temperature dependence of the Raman-scattering spectra in the temperature region from room temperature to 6 K for high-quality crystals of Sr_2RuO_4 with $T_c=1.4$ K, in order to clarify the anisotropic properties of the electron-phonon interaction in the normal phase.

II. EXPERIMENT

Single crystals of Sr_2RuO_4 were grown by a traveling-solvent floating-zone method with an infrared image furnace.¹⁶ For the Raman-scattering measurements, an Ar^+ laser light with a wavelength of 514.5 nm was employed as the incident beam and its output power was 12.5 mW. The scattered light into a nearly backward direction was analyzed by a triple monochromator (JASCO model NR-1800), and the analyzed light was detected by a CCD multi-channel detector (Princeton instrument model LN/CCD-576E).

The Raman-scattering geometry is denoted by the symbol $k_i(p_i, p_s)k_s$, where k and p are the directions of the propagation and polarization of light, respectively, and i and s denote the incident and scattered light, respectively. In this study, three different geometries, $b(a, a)\bar{b}$, $c(a, a)\bar{c}$, and $b(c, c)\bar{b}$ [$=a(c, c)\bar{a}$], with A_{1g} symmetry have been investigated. Here, a , b , and c correspond to the crystallographic axes of [100], [010], and [001], respectively, in the tetragonal symmetry. In these polarization geometries, only two phonon modes are allowed in the tetragonal K_2NiF_4 structure: One corresponds to the in-phase motion between Sr and apical oxygen (P_1) at the energy $\sim 200 \text{ cm}^{-1}$ and the other the apical oxygen vibration (P_2) at $\sim 550 \text{ cm}^{-1}$ along the c axis. We used two surfaces in this study. The b surface was employed for the measurements of $b(c, c)\bar{b}$ and $b(a, a)\bar{b}$, and the c surface for $c(a, a)\bar{c}$. The c surface used was the cleaved surface, while the b surface was polished with an 1 μm diamond slurry and we obtained a similar surface condition to the c surface.

III. RESULTS

Polarization dependence of the Raman spectra is shown in Fig. 1, where (a) is the result for the high-quality crystals with $T_c = 1.4 \text{ K}$ measured at room temperature and (b) is the spectra for the low- T_c crystals with $T_c = 0.97 \text{ K}$ taken at 6 K. Each spectrum is vertically shifted to avoid the crossings, but the zero intensity is depicted by the short horizontal bar at the vertical axis. As shown in Fig. 1, the peaks marked by P_1 and P_2 correspond to the symmetry-allowed vibrations along the c axis in the tetragonal phase. P_1 is the in-phase motion of Sr and apical oxygen, and P_2 the vibration of the apical oxygen. For the low- T_c crystals, we emphasize that the peaks have been clearly observed even at 6 K and the remarkable intensity change of the spectra has not been observed between room temperature and 6 K. The dominant impurities, contained in the low- T_c crystals, were Al with a concentration of 200~300 ppm.¹⁷ However, the high-quality samples clearly show the suppression of the peak intensity of P_2 in both (a, a) spectra. Thus, this intensity change shows that a small amount of impurities smears out the intrinsic properties of Sr_2RuO_4 .

In spite of the equivalent Raman-scattering tensors between $b(a, a)\bar{b}$ and $c(a, a)\bar{c}$, the observed phonon spectra show the following differences for the high-quality samples at room temperature. The line shape of P_2 is highly asymmetric for $b(a, a)\bar{b}$, while that for $c(a, a)\bar{c}$ is almost sym-

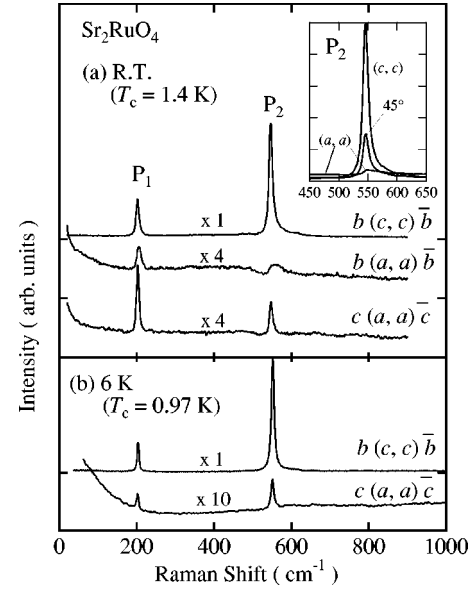


FIG. 1. Polarization dependence of the Raman spectra for Sr_2RuO_4 with (a) the spectrum of the high-quality crystals with $T_c = 1.4 \text{ K}$ taken at room temperature and (b) the spectrum of the crystals with $T_c = 0.97 \text{ K}$ at 6 K. The $b(a, a)\bar{b}$ and $c(a, a)\bar{c}$ spectra in (a) and $c(a, a)\bar{c}$ spectrum in (b) are plotted four and ten times, respectively. The inset shows the polarization dependence from $b(c, c)\bar{b}$ to $b(a, a)\bar{b}$ in the vicinity of P_2 .

metric. Furthermore, the linewidth of P_1 in $b(a, a)\bar{b}$ is almost twice as that in $c(a, a)\bar{c}$, but the integrated intensity of P_1 is almost the same. These remarkable spectral changes originate from the different propagation direction of phonons: The propagation direction of $b(a, a)\bar{b}$ is parallel to the RuO_2 conduction plane and that of $c(a, a)\bar{c}$ is perpendicular to the plane. In general, the optical phonon at the Brillouin-zone center does not depend on the propagation direction. Thus, the present results suggest the existence of an anisotropic interaction with other excitations, such as electronic or magnetic systems, and also the excitations coupled with the phonons strongly depend on the propagation direction and polarization geometry.

The polarization dependence from $b(c, c)\bar{b}$ to $b(a, a)\bar{b}$ in the vicinity of P_2 at room temperature is shown in the inset of Fig. 1, where each spectrum is plotted without the shift along the vertical direction. The distinct difference between $b(c, c)\bar{b}$ and $b(a, a)\bar{b}$ is the decrease in the peak intensity of P_2 and the increase in the background intensity from $b(c, c)\bar{b}$ to $b(a, a)\bar{b}$. Thus, the origin of the background is important for understanding the change in the spectra.

Next, we show the temperature dependence of the Raman-scattering spectra in Fig. 2, where (a), (b), and (c) are the spectra of $b(c, c)\bar{b}$, $b(a, a)\bar{b}$, and $c(a, a)\bar{c}$, respectively. There is no qualitative change in the phonon peaks in the $b(c, c)\bar{b}$ spectrum in this temperature region. However, P_2 in the $b(a, a)\bar{b}$ and $c(a, a)\bar{c}$ spectra shows the difference in temperature dependence from that of $b(c, c)\bar{b}$. The highly asymmetric peak P_2 in $b(a, a)\bar{b}$ is no longer recognized as

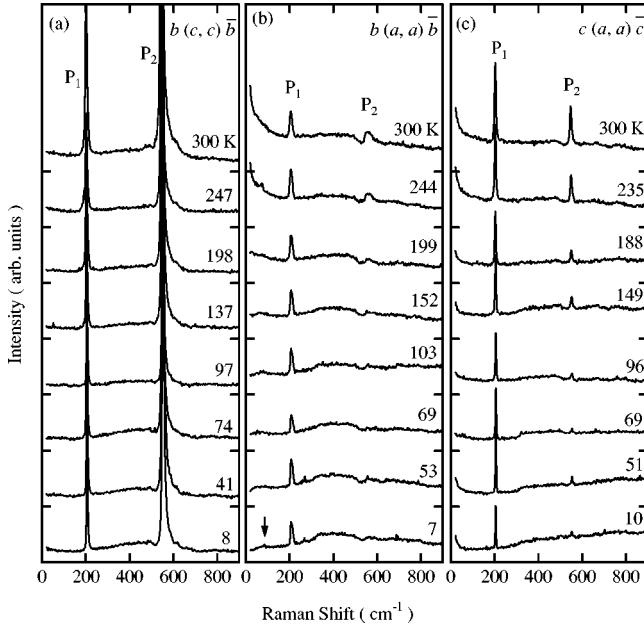


FIG. 2. Temperature dependence of Raman spectra of Sr_2RuO_4 . (a), (b), and (c) are the spectra for the polarization geometries of $b(c,c)\bar{b}$, $b(a,a)\bar{b}$, and $c(a,a)\bar{c}$, respectively. The arrow denotes the spin gap energy. See the text for the details.

the peak below 150 K. Although the intensity of the symmetric peak in the $c(a,a)\bar{c}$ spectrum also decreases, it remains as a very weak peak even at 10 K. To understand such temperature dependence of the intensities quantitatively, the temperature dependence of the energy-integrated intensity ratio $I(P_2)/I(P_1)$ is shown in Fig. 3. We regard that the intensities of P_1 are almost independent of temperature. The broken line denotes the temperature dependence estimated by the Bose-factor correction. In general, the Raman-scattering intensity at the Stokes side is proportional to $n+1$, where n represents the Bose factor. $I(P_2)/I(P_1)$ of $b(c,c)\bar{b}$ is well explained by the Bose-factor correction,¹⁸ however, that of $b(a,a)\bar{b}$ and $c(a,a)\bar{c}$ decreases with a

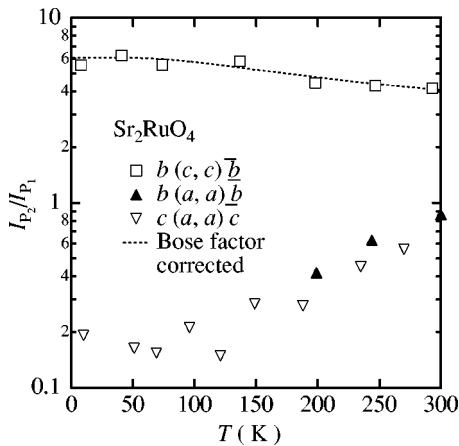


FIG. 3. Temperature dependence of the energy-integrated intensity ratio of $I(P_2)/I(P_1)$. The broken line denotes the temperature dependence estimated by the Bose-factor correction.

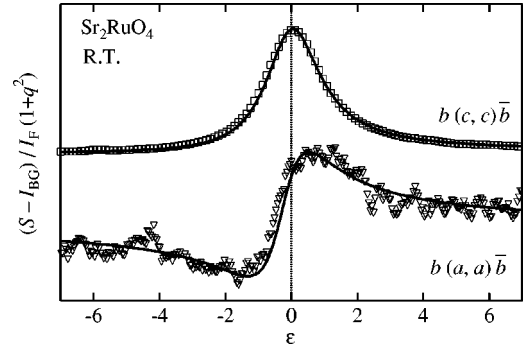


FIG. 4. Representative fitted result at room temperature. Open symbols are the measured data and solid lines are the fitted curve. The vertical axis is normalized by $(S - I_{BG})/I_F(1 + q^2)$ and the horizontal axis is ϵ . The obtained parameters of I_F , ω_p [cm^{-1}], q , Γ [cm^{-1}], and I_{BG} are 0.006 50, 545.9, 12.09, 5.11, and 0.0379 for $c(a,a)\bar{c}$ and 0.010 08, 546.0, 1.20, 12.00, and 0.0486 for $b(a,a)\bar{b}$.

similar gradient with decreasing temperature. Especially in $b(a,a)\bar{b}$, the intensity vanishes below 150 K. Thus, P_2 of the (a,a) geometry is also anomalous in the temperature dependence.

For the background spectra, the bumplike structure from 300 to 600 cm^{-1} becomes apparent and the intensity below 300 cm^{-1} decreases with decreasing temperature for all polarization. Other remarkable changes occur in the low-energy region in $b(a,a)\bar{b}$, where the intensity in the vicinity of 0 cm^{-1} decreases gradually with decreasing temperature, and at 7 K the intensity below 100 cm^{-1} linearly decreases with decreasing energy as depicted by the arrow in Fig. 2.

IV. DISCUSSION

Let us first discuss the line shape of P_2 . As shown in Figs. 1 and 2, the line shape of P_2 is severely asymmetric and is not fitted by the multimode analysis. Here, we have employed the Fano model, which treats the interference effect between a sharp excitation of a phonon and a broad response.^{11,12} The line-shape function S is written as

$$S = I_F \frac{(q + \epsilon)^2}{1 + \epsilon^2} + I_{BG}. \quad (1)$$

The parameters of Eq. (1) have the following relationship with the physical quantities: $I_F = \pi \rho T_e^2$, $q = T_p / \pi \rho V T_e$, and $\epsilon = (\omega - \omega_p) / \Gamma$, where ρ , T_e and T_p , V , ω_p , Γ ($= \pi \rho V^2$), and I_{BG} are the state density of the electronic excitation, the transition probabilities of electronic excitation and phonon, the electron-phonon interaction energy, the phonon energy, the linewidth of the phonon, and the background due to the excitation without coupling to the phonon, respectively. From the line-shape fittings, one set of ω_p , q , Γ , and I_{BG} is derived. The representative fitting result at room temperature is shown in Fig. 4, where solid lines denote the fitted curves and open symbols are the measured data points. In this plot we employ the normalized value by the formula $(S - I_{BG})/I_F(1 + q^2)$ for the vertical axis and ϵ for the hori-

zontal one. The fitting parameters for the spectra presented in Fig. 4 are listed in the caption. The spectrum of $c(a,a)\bar{c}$ was not analyzed by the Fano model, since we regard it as the uncoupled case from its symmetric line shape.

Among q, Γ , and I_F , the most sensitive parameter to the interaction is q , which is often referred to the asymmetric parameter. The increase of the electron-phonon interaction decreases q . Thus, q theoretically becomes infinity for the uncoupled phonon, however, q stays finite in the actual case. In fact, q is at least larger than 100 for $c(a,a)\bar{c}$. The asymmetric parameters for each polarization geometry are summarized as 1.2 for $b(a,a)\bar{b}$, 12.1 for $b(c,c)\bar{b}$, and ≥ 100 for $c(a,a)\bar{c}$ for the data taken at room temperature. The obtained result clearly shows that the phonon propagating along the RuO_2 plane substantially couples with the broad background response, but this is not the case for the perpendicular one. Furthermore, even in the coupled spectrum, the polarization directions parallel to the RuO_2 plane give the stronger electron-phonon interaction [$b(a,a)\bar{b}$ case]. This is understood by the difference in the background intensity, since I_F of $b(c,c)\bar{b}$ is almost half as that for $b(a,a)\bar{b}$ as presented in the caption of Fig. 4. This anomalous polarization dependence of the interaction is caused by the anisotropy due to the highly two-dimensional character of Sr_2RuO_4 .

In the Fano fitting, ρ , T_e , and V are not determined independently. For $\text{La}_{2-x}\text{Sr}_x\text{CuO}_4$, we have succeeded in obtaining the concentration dependence of the electron-phonon interaction in the form of V/T_e , where T_e has been regarded as constant. However, for Sr_2RuO_4 , we do not proceed with a similar discussion, since the transition probability of the electronic system (T_e) cannot be recognized as the same between $b(c,c)\bar{b}$ and $b(a,a)\bar{b}$. We also note that the fitted ω_p converges to the same value of 546 cm^{-1} at room temperature, in spite of the different peak-maximum energy of P_2 between $b(a,a)\bar{b}$, $c(a,a)\bar{c}$, and $b(c,c)\bar{b}$. As pointed out in the previous section, this result shows that the difference in the spectral shape of P_2 is not its own property, that is, the interaction with background is important.

Next we discuss the origin of the background response observed in the wide-energy region. At room temperature, the background intensities of $b(a,a)\bar{b}$ and $c(a,a)\bar{c}$ are similar, but that of $b(c,c)\bar{b}$ is almost half, as shown in Fig. 2, where the horizontal short bar at the vertical axis denotes the origin of the intensity for each shifted spectrum. In Sr_2RuO_4 , the magnetic excitation is possible, since the basic electronic configuration is the low-spin d^4 with the spin of $S=1$ due to Ru. Thus, for the broad response, we can point out the electronic and magnetic excitations as the possible origin. For the $b(c,c)\bar{b}$ spectrum, however, the magnetic excitation is excluded, since the two-magnon excitation is forbidden in a K_2NiF_4 -type structure.¹⁹ Therefore, the background observed in the $b(c,c)\bar{b}$ spectrum is assigned as the electronic one. On the other hand, the spectra of $b(a,a)\bar{b}$ and $c(a,a)\bar{c}$ contain both magnetic and electronic excitations. Thus, the increase in the background intensity of $b(a,a)\bar{b}$ and $c(a,a)\bar{c}$ might

be attributable to the additional contribution of the magnetic excitations. However, it is difficult to obtain the individual contributions precisely, since the transition probabilities of the electronic contribution might be different between $b(c,c)\bar{b}$ and $b(a,a)\bar{b}/c(a,a)\bar{c}$. Therefore, we conclude that the asymmetric line shape of P_2 is caused by the electron-phonon interaction, since the interference effect has been observed even in $b(c,c)\bar{b}$.

Also, the background spectra depend on the temperature. The intensity of $b(c,c)\bar{b}$ corresponding to the electronic excitations is almost temperature independent, while those of $b(a,a)\bar{b}$ and $c(a,a)\bar{c}$ depend on temperature. Especially, intensity less than 300 cm^{-1} remarkably decreases with decreasing temperature for both $b(a,a)\bar{b}$ and $c(a,a)\bar{c}$. According to Katsufuji *et al.*, the in-plane optical conductivity is temperature independent in the normal phase.¹⁴ Thus, we conclude that the electronic contribution of the background does not strongly depend on temperature also in $b(a,a)\bar{b}$ and $c(a,a)\bar{c}$ and the dominant contribution to the temperature dependence is caused by the magnetic excitation. Gap-like spectrum is observed in the energy region less than 100 cm^{-1} only for $b(a,a)\bar{b}$ and becomes clear below 10 K. We assign the origin of the gap spectrum as the spin gap, since its intensity at 20 cm^{-1} between $b(a,a)\bar{b}$ and $b(c,c)\bar{b}$ is almost the same at 7 K and the gaplike spectrum has not been observed in $b(c,c)\bar{b}$. The absence of the gap spectrum in $c(a,a)\bar{c}$ shows that the spin gap appears only for the excitations propagating parallel to the RuO_2 plane and is also highly anisotropic like electronic cases. The obtained experimental evidence suggests that the magnetic excitation is suppressed in the low-temperature region and its low-temperature behavior is important for understanding the mechanism of the superconductivity in Sr_2RuO_4 .

We note again the impurity effect on the electron-phonon interaction in Sr_2RuO_4 . The symmetric line shape of P_2 in the low- T_c sample with $T_c=0.97 \text{ K}$ suggests the electron-phonon interaction of Sr_2RuO_4 is easily suppressed by the introduction of a small amount of impurities. At this stage, it is not clear why the interference effect is easily suppressed by a small amount of impurities.

Finally, we comment on the temperature dependence of the intensity for P_2 . In $b(c,c)\bar{b}$, the intensity ratio of $I(P_2)/I(P_1)$ is well explained by the Bose-factor correction, however, in $b(a,a)\bar{b}$ and $c(a,a)\bar{c}$ this is not the case, as shown in Fig. 3. Especially for $b(a,a)\bar{b}$, P_2 disappears below 150 K. In order to explain the anomalous temperature dependence, we can point out two mechanisms, such as the shielding effect due to carriers as in $\text{La}_2\text{CuO}_{4+\delta}$ (Ref. 18) and the increase of the electron-phonon interaction. However, these mechanisms cannot explain systematically both results of $b(a,a)\bar{b}$ and $c(a,a)\bar{c}$. Thus, the origin of the anomalous temperature dependence remains a question.

In summary, we have found strong propagation dependence of the electron-phonon interaction for the apical vibrations. We found also the suppression of the magnetic excitation at low temperature and the formation of the spin gap

below 100 cm^{-1} at 7 K. The observed spin gap is highly anisotropic, similar to the electronic case. Even in Sr_2RuO_4 , the magnetic correlation is important in understanding the mechanism of superconductivity. Furthermore, the sample quality is crucially important for obtaining the intrinsic physical properties, since the small amount of impurity dramatically changes Raman-scattering spectra.

ACKNOWLEDGMENTS

This work was supported by a Grant-in-Aid for Scientific Research, Japanese Ministry of Education, Science, and Culture. We also acknowledge Professor Katsuhiko Nagai for his valuable discussion. The Raman-scattering experiment was supported by the cryogenic center of Hiroshima University.

*Present address: Tsukuba Magnet Laboratory, National Research Institute for Metals, Tsukuba, Ibaraki 305-0003, Japan.

¹Y. Maeno, H. Hashimoto, K. Yoshida, S. Nishizaki, T. Fujita, J.G. Bednorz, and F. Lichtenberg, *Nature (London)* **372**, 532 (1994).

²T.M. Rice and M. Sigrist, *J. Phys.: Condens. Matter* **7**, L643 (1995).

³K. Ishida, H. Mukuda, Y. Kitaoka, K. Asayama, Z.Q. Mao, Y. Mori, and Y. Maeno, *Nature (London)* **396**, 658 (1998).

⁴G.M. Luke, Y. Fudamoto, K.M. Kojima, M.I. Larkin, J. Merrin, B. Nachumi, Y.J. Uemura, Y. Maeno, Z.Q. Mao, Y. Mori, H. Nakamura, and M. Sigrist, *Nature (London)* **394**, 558 (1998).

⁵R. Jin, Yu. Zadorozhny, D.G. Schlom, Y. Mori, Y. Maeno, and Y. Liu, *Phys. Rev. B* **59**, 4433 (1999).

⁶S. Nishizaki, Z.Q. Mao, and Y. Maeno, *J. Phys. Soc. Jpn.* **69**, 572 (2000).

⁷Z.Q. Mao, Y. Maeno, T. Ando, T. Ishiguro, M. Sigrist, and T. Oguchi, *Phys. Rev. Lett.* **84**, 991 (2000).

⁸M. Udagawa, T. Minami, N. Ogita, Y. Maeno, F. Nakamura, T. Fujita, J.G. Bednorz, and F. Lichtenberg, *Physica B* **219-220**, 222 (1996).

⁹A. Yamanaka, N. Asayama, M. Sasada, K. Inoue, M. Udagawa,

S. Nishizaki, Y. Maeno, and T. Fujita, *Physica C* **263**, 516 (1996).

¹⁰S. Nimori, S. Sakita, N. Ogita, Z.Q. Mao, Y. Maeno, and M. Udagawa, *Physica B* **281-282**, 961 (2000).

¹¹U. Fano, *Phys. Rev.* **124**, 1866 (1961).

¹²K.V. Klein, in *Light Scattering in Solids I*, edited by M. Cardona (Springer-Verlag, Heidelberg, 1983).

¹³S. Nimori, S. Sakita, F. Nakamura, T. Fujita, N. Ogita, and M. Udagawa, *Phys. Rev. B* **62**, 4142 (2000).

¹⁴T. Katsufuji, M. Kasai, and Y. Tokura, *Phys. Rev. Lett.* **76**, 126 (1996). The T_c of the crystal was not mentioned in their paper.

¹⁵M. Braden, W. Rechart, S. Nishizaki, Y. Mori, and Y. Maeno, *Phys. Rev. B* **57**, 1236 (1998).

¹⁶Z.Q. Mao, Y. Maeno, and H. Fukazawa, *Mater. Res. Bull.* **35**, 1813 (2000).

¹⁷A.P. Mackenzie, R.K.W. Haselwimmer, A.W. Tyler, G.G. Lonzarich, Y. Mori, S. Nishizaki, and Y. Maeno, *Phys. Rev. Lett.* **80**, 161 (1998).

¹⁸M. Udagawa, H. Hata, S. Nimori, T. Minami, N. Ogita, S. Sakita, F. Nakamura, T. Fujita, and Y. Maeno, *J. Phys. Soc. Jpn.* **67**, 2529 (1998).

¹⁹J.B. Parkinson, *J. Phys. C* **2**, 2012 (1969).